Spatial persistence and survival probabilities for fluctuating interfaces

M. Constantin*
Condensed Matter Theory Center, Department of Physics, University of Maryland, College Park, Maryland 20742-4111, USA and Materials Research Science and Engineering Center, Department of Physics, University of Maryland, College Park, Maryland 20742-4111, USA

S. Das Sarma and C. Dasgupta†
Condensed Matter Theory Center, Department of Physics, University of Maryland, College Park, Maryland 20742-4111, USA
(Received 18 December 2003; published 13 May 2004)

We report the results of numerical investigations of the steady-state (SS) and finite-initial-conditions (FIC) spatial persistence and survival probabilities for $(1+1)$-dimensional interfaces with dynamics governed by the nonlinear Kardar-Parisi-Zhang equation and the linear Edwards-Wilkinson (EW) equation with both white (uncorrelated) and colored (spatially correlated) noise. We study the effects of a finite sampling distance on the measured spatial persistence probability and show that both SS and FIC persistence probabilities exhibit simple scaling behavior as a function of the system size and the sampling distance. Analytical expressions for the exponents associated with the power-law decay of SS and FIC spatial persistence probabilities of the EW equation with power-law correlated noise are established and numerically verified.

DOI: 10.1103/PhysRevE.69.051603 PACS number(s): 68.37.Ef, 68.35.Ja, 05.20.−y, 05.40.−a

I. INTRODUCTION

The concept of temporal persistence [1], which is closely related to first-passage statistics, has been used recently to study various non-Markovian stochastic processes both theoretically [2,3] and experimentally [4–7]. Another quantity of interest in the study of the statistics of spatially extended systems is its natural analog, the *spatial persistence probability*. This idea has been investigated theoretically [8] in the context of $(d+1)$–dimensional Gaussian interfaces with dynamics described by linear Langevin equations, where the variable undergoing stochastic evolution is the height $h(x,t)$ of the interfacial sites (x is the lateral position along the interface and t is the time). The spatial persistence probability of fluctuating interfaces, denoted by $P(x_0,x_0+x)$, is simply the probability that the height of a steady-state interface configuration, measured at a fixed time t_0, *does not* return to its "original" value $h(x_0,t_0)$ at the initial point x_0 within a distance x measured from x_0 along the interface. In the long-time, steady-state limit, the spatial persistence probability $P(x_0,x_0+x)$, which depends only on x for a translationally invariant interface, has been shown [8] to exhibit a power-law decay, $P(x_0,x_0+x)\sim x^{-\theta}$. One of the interesting results reported in Ref. [8] is that the spatial persistence exponent θ can take two values determined by the initial conditions or selection rules imposed on the starting point x_0: (1) $\theta=\theta_{SS}$, the "steady-state" (SS) persistence exponent if x_0 is sampled uniformly from *all* the sites of a steady-state configuration, and (2) $\theta=\theta_{FIC}$, the so-called *finite-initial-conditions* (FIC) persistence exponent if the sampling of x_0 is performed from a *subset* of steady-state sites where the height variable and its spatial derivatives are *finite*. The spatial persistence probabilities obtained for these two different ways of sampling the initial point are denoted by $P_{SS}(x_0,x_0+x)$ and $P_{FIC}(x_0,x_0+x)$, respectively.

The values of the exponents θ_{SS} and θ_{FIC} for interfaces with dynamics described by a class of linear Langevin equations have been determined in Ref. [8] using a mapping between the spatial statistical properties of the interface in the steady state and the temporal properties of stochastic processes described by a generalized random-walk equation. It turns out that for these systems, θ_{SS} is equal to either $3/2-n$ for $1/2<n<3/2$ or 0 for $n>3/2$, where $n=(z-d+1)/2$, d is the spatial dimension, and z is the standard dynamical exponent of the underlying Langevin equation. The FIC spatial persistence exponent is found to have the value $\theta_{FIC}=\theta(n)$, where $\theta(n)$ is a temporal persistence exponent for the generalized random-walk problem to which the spatial statistics of the interface is mapped. Two exact results for $\theta(n)$ are available in the literature: $\theta(n=1)=1/2$, corresponding to the classical Brownian motion [9] and $\theta(n=2)=1/4$, corresponding to the random acceleration problem [10].

Very recently, experimental measurements of the spatial persistence probability have been performed [7] for a system (combustion fronts in paper) that is believed to belong to the Kardar-Parisi-Zhang (KPZ) [11] universality class. However, the FIC spatial persistence probability is not investigated at all in this work. Instead, the authors analyze a "transient" spatial persistence (i.e., the probability is measured by sampling over all the sites of a transient interfacial profile obtained before the steady state is reached). This transient spatial persistence is completely different from the FIC spatial persistence, which is measured in the steady-state regime by sampling a special class of initial sites. As a consequence, additional study is required in order to understand the experimental and numerical possibilities for measuring P_{FIC} and its associated nontrivial exponent θ_{FIC}.

*Electronic address: mconstan@glue.umd.edu
†Permanent address: Department of Physics, Indian Institute of Science, Bangalore 560012, India.

In this paper, we present the results of a detailed numerical study of spatial persistence in a class of one-dimensional models of fluctuating interfaces. Our interest in analyzing the spatial persistence of fluctuating interfaces is motivated to a large extent by their important (and far from completely understood) role in the rapidly developing field of nanotechnology, where the desired stability of nanodevices requires understanding and controlling thermal interfacial fluctuations. In this context, the study of first-passage statistics in general, or of the persistence probability (both spatial and temporal) [3,8] in particular, turns out to be a very useful approach. To address this problem we consider stochastic interfaces with dynamics governed by the Edwards-Wilkinson (EW) [12] and KPZ equations. For the EW equation, we consider both white noise (uncorrelated in both space and time) and "colored"noise that is correlated in space but uncorrelated in time. The effect of noise in spatially distributed systems is an interesting problem by itself and has been widely studied [13]. In this paper, we investigate the effects of noise statistics on the spatial structure of fluctuating interfaces using the conceptual tool of spatial persistence probability. Using the isomorphic mapping procedure of Ref. [8], we derive exact analytical results for the spatial persistence exponents of $(d+1)$–dimensional EW interfaces driven by power-law correlated noise. We then compare our analytical results with those obtained from numerical integrations of the corresponding stochastic equations. The use of power-law correlated noise in the EW equation allows us to explore the situation where the two spatial persistence exponents θ_{SS} and θ_{FIC} are different.

Our numerical study also provides a characterization of the scaling behavior of spatial persistence probabilities as functions of the system size. Information about the system-size dependence of persistence probabilities is necessary for extracting the persistence exponents from experimental and numerical data. In studies of the scaling behavior of spatial persistence probabilities, one has to consider another important length scale that always appears in practical measurements: this is the *sampling distance* δx which represents the "nearest-neighbor"spacing of the uniform grid of spatial points where the height variable $h(x,t_0)$ is measured at a fixed time t_0. The sampling distance δx is the spatial analog of the "sampling time" [14,15] that represents the time interval between two successive measurements of the height at a fixed position in experimental and computational studies of temporal persistence. Once the effect of a finite δx on the measured spatial persistence is understood, one can relate correctly the experimental and numerical results to the theoretical predictions. Our study shows that the spatial persistence probabilities (both SS and FIC) exhibit simple scaling behavior as functions of the system size and the sampling distance.

In addition to the temporal persistence probability, the temporal survival probability [5,15] has been shown recently to represent an alternative valuable statistical tool for investigations of first-passage properties of spatially extended systems with stochastic evolution. In the context of interface dynamics, the temporal survival probability is defined as the probability that the height of the interface at a fixed position does not cross its *time-averaged* value over time t. In contrast to the power-law behavior of the temporal persistence probability (which, we recall, measures the probability of not returning to the initial position), the temporal survival probability exhibits an exponential decay at long times, providing information about the underlying physical mechanisms and their associated time scales [15]. In this study, we make the first attempt to analyze the behavior of the *spatial survival probability*, $S(x_0,x_0+x)$, defined as the probability of the interface height between points x_0 (which is an arbitrarily chosen initial position) and x_0+x not reaching the average level $\langle h\rangle$ [rather than the original value $h(x_0,t_0)$]. We present numerical results for $S(x_0,x_0+x)$ that show that its spatial behavior in the SS regime is neither power law nor exponential, while in the FIC regime, it becomes very similar to the spatial persistence probability, $P_{FIC}(x_0,x_0+x)$.

The paper is organized as follows. In Sec. II, we define the models studied in this paper, review existing analytical results about their spatial persistence properties, and present new analytical expressions for the spatial persistence exponents for EW interfaces with colored noise in arbitrary spatial dimensions. In Sec. III, we describe the numerical methods used in our study and discuss how the spatial persistence and survival probabilities are measured in our numerical simulations. The results obtained in our $(1+1)$–dimensional numerical investigations are described in detail and discussed in Sec. IV, for both discrete stochastic solid-on-solid models (Sec. IV A) and the spatially discretized EW equation with colored noise (Sec. IV B). Section V contains a summary of the main results and a few concluding remarks.

II. STOCHASTIC EQUATIONS FOR FLUCTUATING INTERFACES

We have performed a detailed numerical study of the spatial persistence of $(1+1)$-dimensional fluctuating interfaces, where the dynamics is described by the well known EW equation

$$\frac{\partial h(x,t)}{\partial t} = \nabla^2 h(x,t) + \eta(x,t), \tag{1}$$

or alternatively by the KPZ equation

$$\frac{\partial h(x,t)}{\partial t} = \nabla^2 h(x,t) + [\nabla h(x,t)]^2 + \eta(x,t), \tag{2}$$

where ∇ and ∇^2 refer to spatial derivatives with respect to x , and $\eta(x,t)$ with $\langle \eta(x,t)\eta(x',t')\rangle \propto \delta(x-x')\delta(t-t')$ is the usual uncorrelated random Gaussian noise. The dynamical exponent for Eq. (1) is $z=2$, and since $d=1$ in our study, the variable n defined in Sec. I is equal to 1. So, we expect both θ_{SS} and θ_{FIC} for this system to be equal to $1/2$ [8]. Although the KPZ equation is nonlinear, characterized by $z=3/2$, it is well known that in the long time limit, the probability distribution of the stochastic height variable $h(x,t)$ in this equation is the same as that in the EW equation **(**i.e. $P(h) \sim \exp[-\int dx(\nabla h)^2]$**)** in $(1+1)$ dimensions. The static roughness exponent, α, is the same $(\alpha=1/2)$ for both cases. The $1+1$–dimensional KPZ model differs from the EW model in

the *transient* scaling regime, where the interfacial roughness grows as a power law in time, but this temporal regime is not involved in the calculation of the spatial persistence probabilities, as explained in Sec. I. As a consequence, the steady-state spatial properties of $(1+1)$-dimensional interfaces governed by Eq. (2) can be mapped, as for Eq. (1), into a stochastic process with $n=1$. So, the expected values of θ_{SS} and θ_{FIC} for the $(1+1)$-dimensional KPZ universality class are also equal to $1/2$. Thus, studies of $(1+1)$-dimensional KPZ and EW interfaces do not bring out the interesting possibility of different values for the spatial persistence exponents θ_{SS} and θ_{FIC}.

To examine the theoretical prediction [8] of a possible difference between the values of θ_{SS} and θ_{FIC}, we consider the case when the interface dynamics is governed by a EW-type equation with long-range spatial correlations in the noise. Specifically, we consider Eq. (1) with Gaussian colored noise [16] with variance given by

$$\langle \eta_c(x,t)\,\eta_c(x',t')\rangle = g_\rho(x-x')\,\delta(t-t'), \tag{3}$$

where $0 \leqslant \rho < 1/2$ is a parameter that characterizes the spatial correlation of the noise, and

$$g_\rho(x-x') = \begin{cases} |x-x'|^{2\rho-1} & \text{if} \quad |x-x'| \neq 0 \\ g_\rho(0) & \text{if} \quad x=x'. \end{cases} \tag{4}$$

We have chosen $g_\rho(0)$ as in Ref. [16] [i.e., $g_\rho(0) = 1/\rho(1/2)^{2\rho}$]. As discussed below, the SS and FIC spatial persistence exponents for $(1+1)$-dimensional interfaces described by the EW equation with this kind of colored noise are expected to be different from one another. This system, thus, provides an opportunity to examine in detail the role of the choice of the initial points in determining the form of the decay of the spatial persistence probability.

By applying the isomorphic mapping recipe of Ref. [8] to the $(d+1)$-dimensional version of Eq. (1) with colored noise η_c whose statistics is defined by Eqs. (3) and (4), we obtain the result, $n=(z-d+1)/2+\rho$ with $z=2$, implying the following analytical expressions for the spatial persistence exponents:

$$\theta_{SS} = \frac{d}{2} - \rho \tag{5}$$

and

$$\theta_{FIC} = \theta\left(\frac{3-d}{2} + \rho\right). \tag{6}$$

Thus, the value of θ_{SS} is completely determined by the noise correlation parameter ρ. However, based on the range of values for ρ, we can only infer that θ_{FIC} varies (presumably in a continuous manner) between $\theta\,(3-d/2)$ and $\theta\,(4-d/2)$ as the parameter ρ is increased from 0 to $1/2$. For $d=1$, this implies a change from the value $\theta(1)=1/2$ to $\theta(3/2)$, expected to lie between 1/2 and $\theta(2)=1/4$, as ρ changes from 0 to $1/2$. Since the value of θ_{SS} for $d=1$ goes to 0 as ρ approaches the value $1/2$, it is clear that the values of the two spatial persistence exponents must be different for a general value of ρ in the range $[0,1/2)$. This difference would be small for ρ near zero (the two persistence exponents have the same value for $\rho=0$), and maximum for ρ near $1/2$. Therefore, the model with ρ substantially different from zero provides a numerically tractable situation where the interesting theoretical prediction of the existence of two different nontrivial spatial persistence exponents can be tested. We also mention that the usual dynamical scaling exponents take the following ρ-dependent values in the model with colored noise: $\alpha=(2-d+2\rho)/2$, $\beta=(2-d+2\rho)/4$. Thus, the general result [8], $\theta_{SS}=1-\alpha$, is satisfied for all d and ρ.

We have investigated these aspects in a detailed numerical study of models that belong in the universality classes of the Langevin equations of Eqs. (1) and (2). For Eq. (1) with uncorrelated white noise, we have used a discrete stochastic solid-on-solid model (the Family model [17]) which is rigorously known to belong to the same dynamical universality class. For Eq. (2) with uncorrelated white noise, we have also used a discrete solid-on-solid model (the Kim-Kosterlitz model [18]). Finally, for the EW equation with colored noise, the numerical results were obtained from a direct numerical integration of the spatially discretized stochastic differential equation.

III. NUMERICAL METHODS

Simulations of the atomistic Family and Kim-Kosterlitz models are carried out using the standard Monte Carlo method for implementing the stochastic deposition rules of each model. Numerical integration of the EW equation with colored noise is performed using the simple Euler method [3,19]. We solve the $(1+1)$–dimensional Eq. (1) with spatially long-range correlated noise for the real variable $h(x_j,t_n)$, where $t_n=n\Delta t$ $(n=0,1,\ldots)$ and $x_j=j\Delta x$ $(j=0,1,\ldots,L-1)$ with periodic boundary conditions. Here, Δt and Δx are the spatial and temporal grid spacings, respectively. Using the forward-time centered-space representation [19], Eq. (1) becomes

$$h(x_j,t_{n+1}) - h(x_j,t_n) = \Delta t\left[\frac{h(x_{j+1},t_n) - 2h(x_j,t_n) + h(x_{j-1},t_n)}{(\Delta x)^2}\right] + \sqrt{\Delta t}\quad \eta_c(x_j,t_n). \tag{7}$$

We have chosen $\Delta x=1$ and Δt small enough (i.e., $\Delta t=0.01$) in order to satisfy the stability criterion $2\Delta t/(\Delta x)^2 \leqslant 1$. The spatial correlation of the noise is given by

$$\langle \eta_c(x_j,t_n)\,\eta_c(x_k,t_m)\rangle = g_\rho(x_j-x_k)\,\delta_{n,m}, \tag{8}$$

with

$$g_\rho(x_j-x_k) = \begin{cases} |x_j-x_k|^{2\rho-1} & \text{if} \quad 1 \leqslant |x_j-x_k| \leqslant \dfrac{L}{2} \\ (L-|x_j-x_k|)^{2\rho-1} & \text{if} \quad |x_j-x_k| > \dfrac{L}{2} \\ g_\rho(0) & \text{if} \quad x_j-x_k=0, \end{cases} \tag{9}$$

where $g_\rho(0)=1/\rho(1/2)^{2\rho}$. The colored noise is generated using the recipe from Ref. [16]. The fast Fourier transform

operation that is used in the noise-generation procedure constrains the system size to be an integral power of 2. Due to the use of periodic boundary conditions [which are also imposed on the noise correlation function, see Eq. (9)], the range of x over which spatial correlations and persistence properties are meaningfully measured is of the order of $L/2$.

The SS spatial persistence probability $P_{SS}(x_0,x_0+x)$ is measured at a fixed time t_0 (which is much larger than the time $t_{sat}\sim L^z$ required for the interface roughness to saturate) as the probability that the interface height variable does not cross its value, $h(x_0,t_0)$, at the initial point x_0 as one moves along the interface from the point x_0 to the point x_0+x. This probability is averaged over all the sites in a steady-state configuration and also over many independent realizations of the stochastic evolution. Thus,

$$P_{SS}(x_0,x_0+x) \equiv \mathrm{Prob}\{\mathrm{sgn}[h(x_0+x')-h(x_0)] = \mathrm{const}, \quad \forall\, 0<x'\leqslant x, \forall\, x_0\in \mathcal{S}_{SS}\}, \tag{10}$$

where $\mathrm{sgn}[y]$ represents the sign of the fluctuating quantity y, and $\mathcal{S}_{SS}$ is the ensemble containing all the lattice sites in a steady-state configuration. The FIC spatial persistence probability $P_{FIC}(x_0,x_0+x)$ is obtained in a similar manner, except that the average is performed over a particular subensemble of the steady-state configuration sites, $\mathcal{S}_{FIC}\subset\mathcal{S}_{SS}$, characterized by *finite* values of the height variable and its spatial derivatives:

$$P_{FIC}(x_0,x_0+x) \equiv \mathrm{Prob}\{\mathrm{sgn}[h(x_0+x')-h(x_0)] = \mathrm{const}, \quad \forall\, 0<x'\leqslant x, \forall\, x_0\in \mathcal{S}_{FIC}\}. \tag{11}$$

Since the persistence probabilities are averaged over the choice of the initial point x_0, we omit writing x_0 explicitly in the arguments of P_{SS} and P_{FIC} from now on, while stressing the important fact that the ensemble of initial sites used in the averaging process determines which one of the two persistence probabilities is obtained. We consider two different methods for measuring $P_{FIC}(x)$, depending on the type of the model (atomistic solid-on-solid model or spatially discretized Langevin equation) being studied. In the former case where the height variables are integers, the FIC spatial persistence probability measurement involves a sampling procedure from the subset of sites characterized by a fixed integer value of the height (measured from the average, $\langle h\rangle$, of the heights of all the sites at time t_0) which is substantially smaller than the typical value of the height fluctuations measured by the saturation width of the interface profile. In calculations using the direct numerical integration technique, the height variable can take any real value. So, the probability of finding a fixed value of the stochastic height variable is infinitesimally small. For this reason, fixing a reference level H and sampling over the sites with $h(x_0,t_0)=\langle h\rangle+H$ is useless. We, therefore, consider in this case a continuous interval of height values (symmetric with respect to the average height $\langle h\rangle$) with width w, which is considerably smaller than the amplitude of the height fluctuations. The positions characterized by a height variable within this interval represent the subensemble of lattice positions involved in the sampling procedure necessary for measuring $P_{FIC}(x)$.

The spatial survival probabilities corresponding to the SS and FIC conditions are calculated similarly to the corresponding persistence probabilities, except that the stochastic variable under consideration becomes $h(x_0+x')-\langle h\rangle$. Thus,

$$S_{SS}(x_0,x_0+x) \equiv \mathrm{Prob}\{\mathrm{sgn}[h(x_0+x')-\langle h\rangle] = \mathrm{const}, \quad \forall\, 0\leqslant x'\leqslant x, \forall\, x_0\in \mathcal{S}_{SS}\} \tag{12}$$

and

$$S_{FIC}(x_0,x_0+x) \equiv \mathrm{Prob}\{\mathrm{sgn}[h(x_0+x')-\langle h\rangle] = \mathrm{const}, \quad \forall\, 0\leqslant x'\leqslant x, \forall\, x_0\in \mathcal{S}_{FIC}\}. \tag{13}$$

IV. RESULTS AND DISCUSSIONS

A. Solid-on-solid models

In the solid-on-solid Family and Kim-Kosterlitz models, the interface configuration is characterized by a set of integer height variables $\{h_i\}_{i=1,L}$ corresponding to the lattice sites $i=1,\ldots,L$, with periodic boundary conditions. Since all the measurements of the spatial persistence and survival probabilities are done in the steady-state regime (i.e., in the regime where the interfacial roughness has reached a time-independent saturation value), we used relatively small systems with $L\sim 200-3000$ in order to be able to achieve the the steady state within reasonable simulation times. The resulting steady-state interfacial profile, corresponding to a final time $t_0>>L^z$, is used to compute the spatial persistence and survival probabilities. The calculation of $P_{SS}(x)$ is relatively simple: it involves measuring the fraction of initial lattice positions (all possible choices of the initial point are allowed) for which the interface height has not returned to the height of the initial point (for persistence probability) or to the average height level $\langle h\rangle$ (for survival probability) over a distance x, averaged over many independent realizations ($\sim 10^3-10^4$) of the steady state configuration. Measurements of $P_{FIC}(x)$ or $S_{FIC}(x)$ involve, in addition to these steps, a preliminary selection of a subensemble of lattice sites which are characterized by a fixed and small value H of the height measured relative to the spatial average. Only the sites that belong to this subensemble (i.e., only the sites with $h_i=H+\langle h\rangle$) are used as initial points in the FIC measurements.

Two distinct length scales have to be taken into consideration in the interpretation of the numerical results for the spatial persistence probability: the size L of the sample used in the simulation, and the sampling distance δx which denotes the spacing between two successive points where the height variables are measured in the calculation of the persistence probability. The minimum value of δx is obviously one lattice spacing, but one can use a larger integral value of δx in the calculation of persistence and survival probabilities. For example, a calculation of the persistence probability with $\delta x=m$ would correspond to checking the heights of only the sites with index i_0+jm, where i_0 is the index of the initial site and $j=1,2,\ldots$. While the importance of L in the measure-

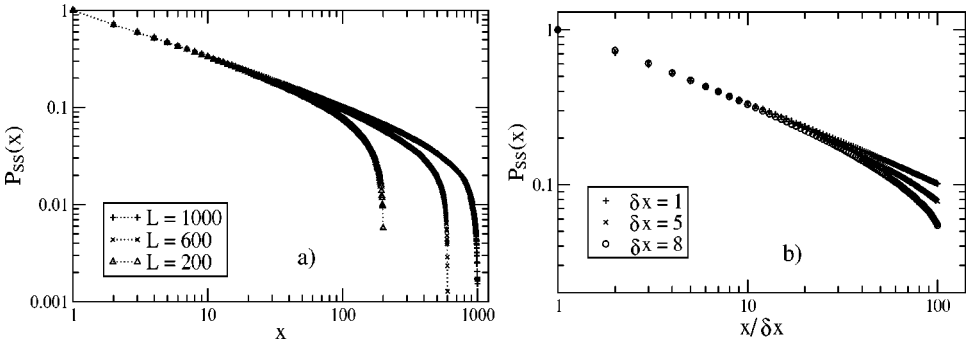

FIG. 1. The steady state spatial persistence probability, $P_{SS}(x)$, for $(1+1)$-dimensional EW interfaces with white noise, obtained using the discrete Family model. Panel (a): Double-log plots of $P_{SS}(x)$ vs x for a fixed sampling distance $\delta x=1$, using three different values of L, as indicated in the legend. Panel (b): Double-log plots of $P_{SS}(x)$ vs $x/\delta x$ for a fixed system size, $L=1000$, and three different values of δx, as indicated in the legend.

ment of $P(x)$ is obvious (it sets the maximum distance for which $P(x)$ can be meaningfully measured), the effect of δx is rather intricate and has to be carefully investigated. In Fig. 1(a), we start to analyze these effects by looking at $P_{SS}(x)$ for EW-type interfaces. We note that when $P_{SS}(x)$ is measured in systems with different sizes, using the smallest possible value for δx (i.e., $\delta x=1$), the exponent associated with the power-law decay of the persistence probability does not change, but there is an abrupt downward departure from a power-law behavior near $x=L/2$. It is not difficult to understand this behavior qualitatively: as discussed earlier, measurements of spatial correlations and persistence probabilities in a finite system of size L with periodic boundary conditions are meaningful only for distances smaller than $L/2$. In Fig. 1(b), we have shown the results for $P_{SS}(x)$ when L remains fixed and δx is varied. Since the the persistence probability is, by definition, equal to unity for $x=\delta x$ [see Eq. (10)], we have plotted P_{SS} as a function of $x/\delta x$ in this figure to ensure that the plots for different values of δx coincide for small values of the x coordinate. The plots for different δx are found to splay away from each other at large values of $x/\delta x$, with the plots for larger δx exhibiting more pronounced downward bending. Again, the reason for this behavior is qualitatively clear: since a double-log plot of $P_{SS}(x)$ vs x begins to deviate substantially from linearity as x approaches $L/2$ [see Fig. 1(a)], the downward bending of the plots in Fig. 1(b) (which are all for a fixed value of L) occurs at a smaller value of $x/\delta x$ for larger δx. A more detailed scaling analysis of the dependence of the persistence probabilities on x and δx is described below.

In Fig. 2, we show the results for spatial persistence and survival probabilities for the discrete Family model. It is obvious from the plots that the spatial persistence probabilities $P_{SS}(x)$ [panel (a)] and $P_{FIC}(x)$ [panel (c)] exhibit power-law decays over an extended range of x values. The abrupt decay to zero near $x=L/2$ is due, as discussed above, to finite size effects. The spatial persistence exponents are extracted from the power-law fits shown in the log-log plots as dashed straight lines. We find that $\theta_{SS}\simeq 0.51$, is in good agreement with the expected value $1/2$. However, it is clear that the steady-state survival probability $S_{SS}(x)$, shown in Fig. 2(a), does not exhibit a power-law behavior. This is similar to the qualitative behavior of the *temporal* survival probability in the steady state of the Family model [15].

We now return to the dependence of the persistence probabilities on the sample size L and the sampling distance δx. Since L and δx are the only two length scales in the problem (the lattice parameter serves as the unit of length), it is reasonable to expect [15] that the persistence probabilities would be functions of the (dimensionless) scaling variables x/L and $\delta x/L$. If this is true, then plots of P vs x/L for different sample sizes should show a scaling collapse if the ratio $\delta x/L$ is kept constant. A similar scaling behavior of the temporal survival probability as functions of L and the sampling time δt (in that case, the scaling variables are t/L^z and $\delta t/L^z$) was found in Ref. [15]. As indicated in panels (b-d) of Fig. 2, we have used various values for the sampling distance δx in the measurement of $P_{SS}(x)$ and $P_{FIC}(x)$. We observe that when the sampling distance is increased in proportion to the system size (so that $\delta x/L$ is held fixed), all the $P_{SS}(x)$ curves collapse when plotted vs x/L [see panel (b)]. This confirms that the scaling form of the steady-state persistence probability is:

$$P_{SS}(x,L,\delta x) = f_1(x/L,\delta x/L), \tag{14}$$

where the function $f_1(x_1,x_2)$ shows a power-law decay with exponent θ_{SS} as a function of x_1 for small values of x_1 and $x_2 \ll 1$.

Let us turn our attention to $P_{FIC}(x)$. In the data shown in panel (c) of Fig. 2, we have chosen the subensemble $\mathcal{S}_{FIC}$ of sampling positions to contain only the lattice sites whose height h_i is equal to the average value $\langle h\rangle$ (i.e., $H=0$). Obviously, in this case the definitions for persistence and survival probabilities become identical, since the probability that the height variable does not return to the original value (i.e., $h_i = \langle h\rangle$) is precisely the probability that the height variable does not reach the average level $\langle h\rangle$. We find that $\theta_{FIC} \simeq 0.48$ using a system with $L=1000$ and $\delta x=1$ and considering the subensemble of sites with $H=0$. We note that a remarkable collapse of $P_{FIC}(x)$ vs x/L curves for different values of L is again obtained when δx is adjusted to be proportional to the system size L, as shown in panel (c). More interestingly, we observe that fixing the level H to a

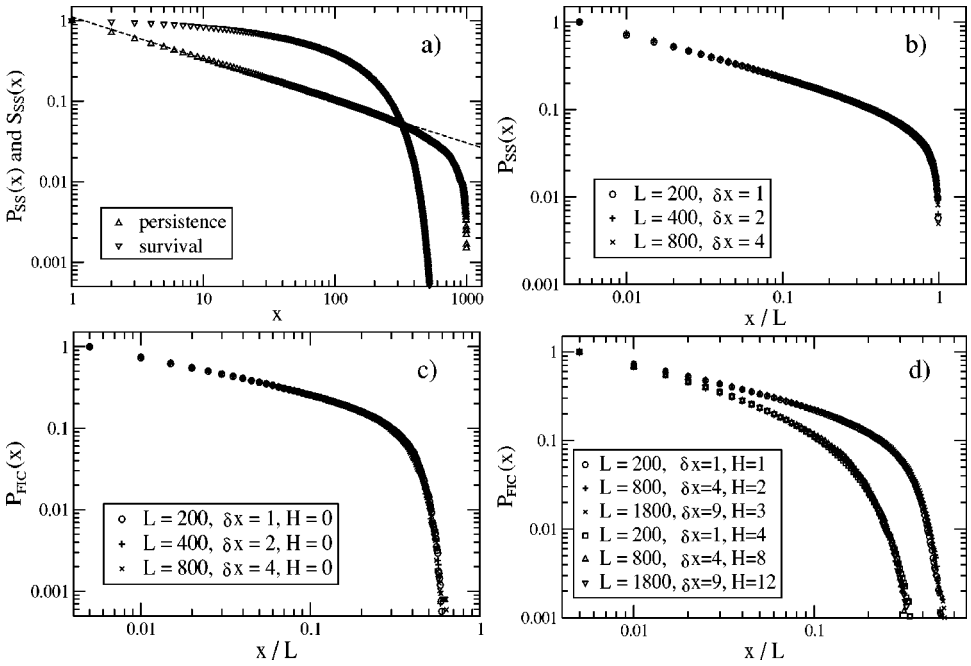

FIG. 2. The spatial persistence probabilities, $P_{SS}(x)$ and $P_{FIC}(x)$, and the spatial survival probability, $S_{SS}(x)$, obtained from simulations of the Family model in $(1+1)$ dimensions. In panels (a) and (b) we show the data for $P_{SS}(x)$ and $S_{SS}(x)$, while in panels (c) and (d) we display the data for $P_{FIC}(x)$. Panel (a): $P_{SS}(x)$ and $S_{SS}(x)$ for $L=1000$, $\delta x=1$. The dashed line represents the best fit of the $P_{SS}(x)$ data to a power-law form. Panel (b): Finite-size scaling of $P_{SS}(x,L,\delta x)$. Three probability curves are obtained for three different sample sizes with the same value for the ratio $\delta x/L=1/200$. Panel (c): Scaling of $P_{FIC}(x,L,\delta x,H)$ for the same values of L and δx as in panel (b). P_{FIC} is calculated by sampling over lattice sites with $H=0$. Panel (d): Scaling of $P_{FIC}(x,L,\delta x,H)$ for three different sample sizes with the same value for the ratio $\delta x/L$, sampling over two subsets of lattice sites with the same value of $H/L^{\alpha}(\alpha=0.5)$: $1/\sqrt{200}$ (upper plot) and $4/\sqrt{200}$ (lower plot).

nonzero value introduces a "height" scale in the problem that is related to the steady-state value of the interface width. Since this width is proportional to L^{α}, where α is the roughness exponent, we expect the dependence of P_{FIC} on H for nonzero values of H to be described by the scaling variable H/L^{α}. We observe that if the level H is chosen to be proportional to L^{α}, then the calculated values of P_{FIC} for different sample sizes, obtained using values of δx such that the ratio $\delta x/L$ is also held constant, exhibit a perfect scaling collapse, as shown in panel (d) of Fig. 2. This observation leads us to the conclusion that the scaling form of the FIC persistence probability with nonzero values of the level H is

$$P_{FIC}(x,L,\delta x,H) = f_2(x/L,\delta x/L,H/L^{\alpha}), \tag{15}$$

where $f_2(x_1,x_2,x_3)$ exhibits a power-law behavior with exponent θ_{FIC} as a function of x_1 for small x_1 if $x_2 \ll 1$ and $x_3 \to 0$. As the value of x_3 is increased, the range of x_1 values over which the power-law behavior is obtained decreases and a more rapid decay of the probability is noticed.

The predictions concerning the scaling behavior of the spatial persistence probabilities are confirmed by the results for the atomistic Kim–Kosterlitz model. The same discussion for Fig. 2 applies to Fig. 3, where we have shown the results for the Kim-Kosterlitz model. We find that $\theta_{SS} \simeq 0.52$ [see Fig. 3(a)], in good agreement with the expected value of $1/2$, and also that $\theta_{FIC} \simeq 0.47$, using a rather small simulation with $L=300$ and $\delta x=1$ and sampling over the subensemble of sites with height at the average level [see Fig. 3(c)]. As shown in Fig. 3(b), the SS persistence probability obeys the scaling form of Eq. (14). In Fig. 3(d), we display the results for the measured P_{FIC} for systems with different sizes and sampling distances such that $\delta x/L$ remains constant and considering two different subsets of sampling sites, each subset being characterized by a fixed value of H/L^{α}. These results are in perfect agreement with the scaling form of Eq. (15).

Equations (14) and (15) provide a complete scaling description of the SS and FIC persistence probabilities for $(1+1)$-dimensional fluctuating interfaces belonging to two different universality classes (i.e., EW and KPZ), modeled using discrete solid-on-solid models. The associated spatial persistence exponents θ_{SS} and θ_{FIC} are in good agreement with the theoretical values [8]. However, these studies do not illustrate the interesting possibility of a dependence of the persistence exponent on the sampling procedure used in the selection of the initial sites used in the calculation of the persistence probability: the two persistence exponents θ_{SS} and θ_{FIC} have the same value for $(1+1)$-dimensional EW and KPZ interfaces. We present and discuss below the results for a model where these two exponents have different values.

B. EW equation with colored noise

In order to measure the spatial persistence and survival probabilities in this system, we have applied the steps described above on systems of sizes $\sim 2^8 - 2^{10}$, using 100–400 independent realizations for averages. While the calculation of $P_{SS}(x)$ and $S_{SS}(x)$ involves the same method as the one

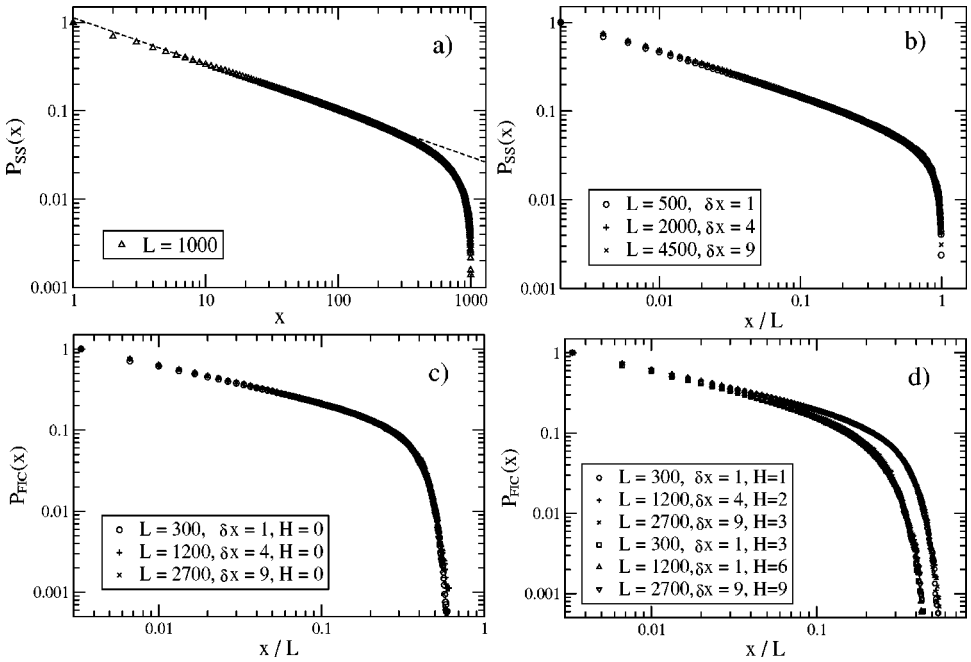

FIG. 3. The spatial persistence probabilities, $P_{SS}(x)$ and $P_{FIC}(x)$, for the (1+1)-dimensional Kim-Kosterlitz model which is in the KPZ universality class. As in Fig. 2, in panels (a) and (b) we show the data for $P_{SS}(x)$. Panels (c) and (d) display the data for $P_{FIC}(x)$. Panel (a): $P_{SS}(x)$ for $L=1000$, $\delta x=1$. Panel (b): Finite-size scaling of $P_{SS}(x,L,\delta x)$. Three probability curves are obtained for three different sample sizes with the same value for the ratio $\delta x/L=1/500$. Panel (c): Scaling of $P_{FIC}(x,L,\delta x,H)$, obtained by sampling over the lattice sites with $H=0$, for three different values [same as those in panel (b)] of L and δx. Panel (d): Scaling of $P_{FIC}(x,L,\delta x,H)$ for three different sample sizes with the same value for the ratio $\delta x/L$, sampling over two subsets of lattice sites with the same value of $H/L^{\alpha}(\alpha=0.5)$: $1/\sqrt{300}$ (upper plot) and $3/\sqrt{300}$ (lower plot).

used in the case of the solid-on-solid models, for measuring $P_{FIC}(x)$ and $S_{FIC}(x)$ we have selected the subensemble of lattice sites whose heights $h(x_j,t_0)$ at time $t_0 \gg L^z$ satisfy the condition $\langle h\rangle - w/2 \leqslant h(x_j,t_0) \leqslant \langle h\rangle + w/2$, where $\langle h\rangle$ is the spatial average of the height at time t_0. The width w of the sampling window has to be chosen to be much smaller than the amplitude of the interface fluctuations, but large enough to include a relatively large fraction of the total number of sites in order to ensure adequate statistics. Under these circumstances we have computed the fraction of these selected sites which do not reach the "original" height $h(x_j,t_0)$ (in the case of persistence probability) or the average height level $\langle h\rangle$ (in the case of survival probability) up to a distance x from the point x_j. The numerical results for these probabilities, along with a finite-size scaling analysis of their behavior, are shown in Figs. 4 and 5.

We find that both SS and FIC spatial persistence probabilities for (1+1)-dimensional interfaces described by the EW equation with colored noise exhibit the expected power-law behavior as a function of x, as shown in Fig. 4, while the SS survival probability shows a more complex x dependence [see Fig. 4(a)]. Further work is needed in order to understand the behavior of $S_{SS}(x)$. When a relatively small system with size $L=2^9$ is used, the numerical results for the spatial per-

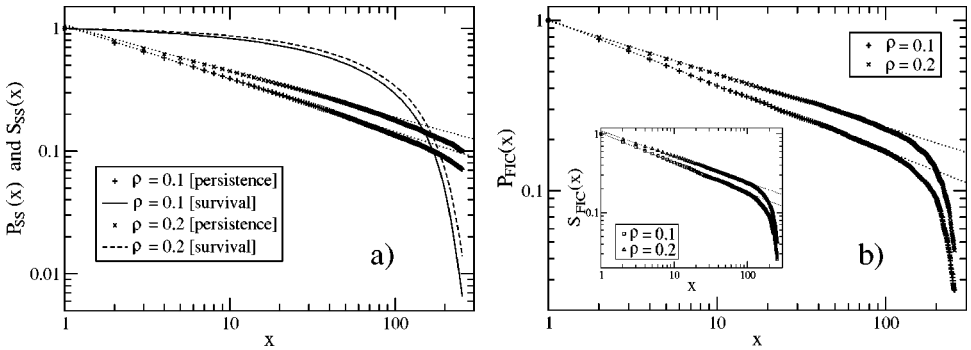

FIG. 4. Spatial persistence and survival probabilities for the EW equation with spatially correlated noise. Panel (a): $P_{SS}(x)$ and $S_{SS}(x)$ using a fixed system size $L=2^9$, two values of the noise correlation parameter ($\rho=0.1$ and 0.2) and sampling distance $\delta x=1$. Panel (b): $P_{FIC}(x)$ and $S_{FIC}(x)$ (inset), using the same parameters as in panel (a), and sampling initial sites from a band of width $w=0.10$ centered at the average height. The straight lines drawn through the data points in these double-log plots represent power-law fits.

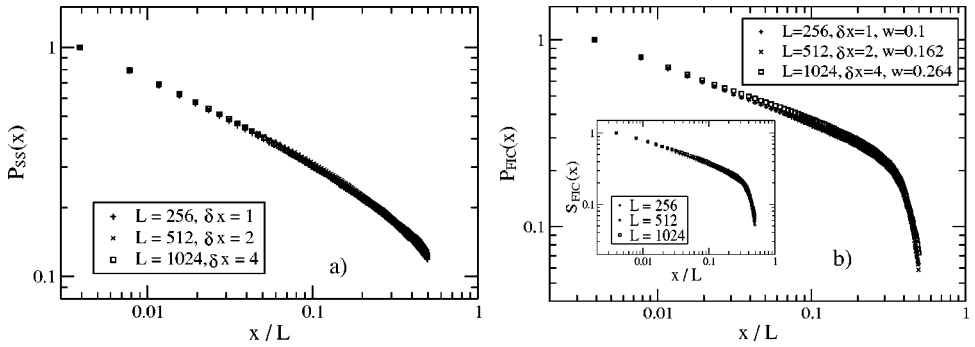

FIG. 5. Finite-size scaling of the persistence probabilities, $P_{SS}(x)$ and $P_{FIC}(x)$, and the FIC survival probability $S_{FIC}(x)$ for the EW equation with spatially correlated noise. The noise correlation parameter is $\rho=0.2$ and the sampling interval δx takes three different values. Panel (a): The SS persistence probability $P_{SS}(x,L,\delta x)$ for three different sample sizes with a constant ratio $\delta x/L=1/2^8$. Panel (b): The FIC persistence probability $P_{FIC}(x,L,\delta x,w)$ with fixed values of the quantities $\delta x/L$ $(=1/2^8)$ and w/L^{α} $(=0.1/2^{5.6})$, where $\alpha=0.7$. Inset: Same as in the main figure, but for the FIC survival probability $S_{FIC}(x,L,\delta x,w)$.

sistence exponents extracted from the power-law fits shown in Fig. 4 (for $\rho=0.1$, we obtain $\theta_{SS}\simeq 0.43$ and $\theta_{FIC}\simeq 0.38$, while for $\rho=0.2$, the exponent values are found to be $\theta_{SS}\simeq 0.37$ and $\theta_{FIC}\simeq 0.31$) appear to be affected by finite-size effects. Specifically, the values of θ_{SS} extracted from fits to the numerical data are systematically larger than the theoretically expected values, $\theta_{SS}=0.4$ for $\rho=0.1$ and 0.3 for $\rho=0.2$ [see Eq. (5)]. Similar deviations from the analytical results are also found for the usual dynamical scaling exponents α and β. We have checked that simulations of larger samples bring the measured values of the exponents closer to the expected values, but the convergence is rather slow. These finite-size effects become more pronounced as the noise correlation parameter ρ is increased. In Fig. 4, we show the results for $\rho=0.1$ and $\rho=0.2$, but we have verified from simulations with larger values of ρ that the difference between the expected and measured values of θ_{SS} increases as ρ is increased. This is expected because the spatial correlation of the noise falls off more slowly with distance as ρ is increased, thereby making finite-size effects more pronounced. Another possible source of the discrepancy between the numerical and exact results for the exponent θ_{SS} is the spatial discretization used in the numerical work. The effects of using a finite discretization scale Δx on the observed scaling behavior of continuum growth equations in the steady state have been studied in Ref. [20], where it was found that the effective value of the roughness exponent α obtained from calculations of the local width using a finite Δx is smaller than its actual value. Since $\theta_{SS}=1-\alpha$, the values of θ_{SS} obtained from our calculations with $\Delta x=1$ are expected to be larger than their exact values. Our results are consistent with this expectation. As shown in the inset of Fig. 4(b), the FIC survival probability $S_{FIC}(x)$ behaves similarly to $P_{FIC}(x)$ for both $\rho=0.1$ and 0.2, exhibiting a power-law decay with an exponent (of 0.38 and 0.33 for $\rho=0.1$ and 0.2, respectively) that is very close to θ_{FIC}. This is consistent with the expectation that the FIC persistence and survival probabilities should become identical as the width parameter w used in the selection of initial sites approaches zero (in this limit, both persistence and survival probabilities measure the probability of not crossing the average height). Finally, we point out that both SS and FIC exponents obtained from the numerical study exhibit the correct trend, increasing in magnitude as ρ decreases. Also, the measured FIC spatial persistence exponents satisfy the constraint $1/4<\theta_{FIC}\leqslant 1/2$. Our numerical results also confirm the interesting theoretical prediction that the SS and FIC spatial persistence exponents are different for the EW equation with spatially correlated noise.

We have found that the scaling forms of Eqs. (14) and (15) also provide a correct description of the numerically obtained persistence and survival probabilities for the EW equation with spatially correlated noise. This is illustrated in Fig. 5. In Fig. 5(a), we show that the results for $P_{SS}(x,L,\delta x)$ obtained for different values of L and δx fall on the same scaling curve when plotted against x/L if the ratio $\delta x/L$ is held fixed. This is precisely the behavior predicted by Eq. (14). As shown in Fig. 5(b), the data for $P_{FIC}(x,L,\delta x,w)$ also exhibit good finite-size scaling collapse if δx is varied in proportion to L and the width w of the sampling band is increased in proportion to L^{α}. This is in perfect analogy with the scaling behavior of the FIC persistence probability for the discrete stochastic models discussed in Sec. IV A, with the variable w playing the role of H in Eq. (15). This suggests that the scaling behavior of the FIC persistence probability in the continuum EW equation is of the form

$$P_{FIC}(x,L,\delta x,w)=f_3(x/L,\delta x/L,w/L^{\alpha}), \tag{16}$$

where the function f_3 has the same characteristics as f_2 in Eq. (15). A similar scaling description also applies to $S_{FIC}(x)$, as shown in the inset of Fig. 5(b). This scaling description should be useful in the analysis of experimental data on equilibrium step fluctuations [5,6] because the images obtained in experiments provide the values of a real "height" variable (position of a step-edge) at discrete intervals of a finite sampling distance δx.

V. SUMMARY AND CONCLUDING REMARKS

In this study, we have analyzed the spatial first-passage statistics of fluctuating interfaces using the concepts of spatial persistence and survival probabilities. Specifically, we have presented the results of detailed numerical measurements of the SS and FIC spatial persistence probabilities for

several models of interface fluctuations. Results for the spatial survival probabilities are also reported. These results confirm that the concepts of persistence and survival are useful in analyzing the spatial structure of fluctuating interfaces. The exponents associated with the power-law decay of the spatial persistence probabilities as a function of distance x are valuable indicators of the universality class of the stochastic processes that describe the dynamics of surface fluctuations. Our results for these exponents for $(1+1)$-dimensional interfaces in the EW and KPZ universality classes are in good agreement with the corresponding analytic predictions. We have also obtained analytic results for the spatial persistence exponents in the $(1+1)$-dimensional EW equation with spatially correlated noise, and reported the results of a numerical calculation of the persistence and survival probabilities in this system. While the numerical results show strong finite-size effects, the qualitative trends predicted by the analytic treatment are confirmed in the numerical work. In particular, the numerical results show evidence for an interesting, theoretically predicted difference between the persistence exponents obtained for two different ways of sampling the initial points used in the measurement of the spatial persistence probability. We also find that the steady-state survival probability has a complex spatial behavior that requires further investigations. In the past, there has been some confusion in the literature about the distinction between the persistence and survival probabilities [15]. Our study shows that these two quantities are very different in the SS situation, whereas the distinction between them essentially disappears in the FIC situation.

The numerical results reported here are for models that exhibit "normal" scaling behavior with the same local and global scaling properties of interface fluctuations. There are other models of interface growth and fluctuations that exhibit "anomalous" scaling [21], for which the global and local scaling properties are different. In such models, the "global" roughness exponent α_g that describes the dependence of the interface width in the steady state on the sample size L ($W(t_0,L) \propto L^{\alpha_g}$ for $t_0 \gg L^z$) is different from the "local" exponent α_l that describes the x dependence of the height-difference correlation function $g(x) \equiv \langle [h(x+x_0,t_0) - h(x_0,t_0)]^2 \rangle^{1/2}$ in the steady state ($t_0 \gg L^z$) for small x ($g(x) \propto x^{\alpha_l}$ for $x \ll L$). The exponent α_g is greater than unity (the steady-state interface is "super-rough") in such cases, whereas the local exponent α_l is always less than or equal to unity. It is interesting to enquire about the behavior of the spatial persistence probabilities in such models. The numerical results reported in the preceding sections show that the steady-state persistence probability $P_{SS}(x)$ exhibits a power-law decay in x only for values of x that are much smaller than the sample size L. Since the roughness of the steady-state interface of super-rough models at length scales much smaller than L is described by the local exponent α_l, we expect the steady-state spatial persistence probability in such models to exhibit a power-law decay with exponent $\theta_{SS} = 1 - \alpha_l$ for $x \ll L$. For example, the one-dimensional Mullins-Herring model [22] is super-rough with $\alpha_g = 3/2$ and $\alpha_l = 1$. For this model, the above argument suggests that the steady-state spatial persistence exponent θ_{SS} is equal to 0, which agrees with the exact result reported in Ref. [8].

An important feature of our investigation is the development of a scaling description of the effects of a finite system size and a finite sampling distance on the measured persistence probabilities. We have also shown that the dependence of the FIC persistence and survival probabilities on the reference level H (in atomistic models) or the width w of the band (in continuum models) used in the selection of the subset of sampling sites is described by a scaling form. These scaling descriptions would be useful in the analysis of experimental and numerical data on fluctuations in spatially extended stochastic systems.

Some of the numerical results reported here (such as the behavior of the SS survival probability and the forms of the scaling functions that describe the dependence of the persistence probabilities on the parameters L, δx, and H or w) should be amenable to analytic treatment, especially for the EW equation with white noise, whose spatial properties can be mapped [8] to the temporal properties of the well-known random-walk problem. Further work along these lines would be very interesting. The spatial persistence and survival probabilities considered here should be measurable in imaging experiments on step fluctuations [5,6]. Such experimental investigations would be most welcome.

ACKNOWLEDGMENTS

This work is partially supported by the US-ONR, the LPS, and the NSF-DMR-MRSEC at the University of Maryland. The authors would like to thank Satya N. Majumdar for several useful discussions. M.C. acknowledges useful discussions with E.D. Williams and D.B. Dougherty.

[1] For a review on temporal persistence, see S. N. Majumdar, Curr. Sci. **77**, 370 (1999).

[2] S. N. Majumdar, C. Sire, A. J. Bray, and S. J. Cornell, Phys. Rev. Lett. **77**, 2867 (1996); B. Derrida, V. Hakim, and R. Zeitak, *ibid.* **77**, 2871 (1996).

[3] J. Krug, H. Kallabis, S. N. Majumdar, S. J. Cornell, A. J. Bray, and C. Sire, Phys. Rev. E **56**, 2702 (1997); H. Kallabis and J. Krug, Europhys. Lett. **45**, 20 (1999).

[4] M. Marcos-Martin, D. Beysens, J. P. Bouchaud, C. Godreche, and I. Yekutieli, Physica A **214**, 396 (1995); W. Y. Tam, R. Zeitak, K. Y. Szeto, and J. Stavans, Phys. Rev. Lett. **78**, 1588 (1997); B. Yurke, A. N. Pargellis, S. N. Majumdar, and C. Sire, Phys. Rev. E **56**, R40 (1997); G. P. Wong, R. W. Mair, R. L. Walsworth, and D. G. Cory, Phys. Rev. Lett. **86**, 4156 (2001).

[5] D. B. Dougherty, I. Lyubinetsky, E. D. Williams, M. Constantin, C. Dasgupta, and S. Das Sarma, Phys. Rev. Lett. **89**, 136102 (2002).

[6] D. B. Dougherty, O. Bondarchuk, M. Degawa, and E. D. Wil-

liams, Surf. Sci. **527**, L213 (2003).
[7] J. Merikoski, J. Maunuksela, M. Myllys, J. Timonen, and M. J. Alava, Phys. Rev. Lett. **90**, 024501 (2003).
[8] S. N. Majumdar and A. J. Bray, Phys. Rev. Lett. **86**, 3700 (2001).
[9] W. Feller, *Introduction to Probability Theory and Its Applications*, 3rd ed. Vol.1 (Wiley, New York, 1968).
[10] T. W. Burkhardt, J. Phys. A **26**, L1157 (1993); Y. G. Sinai, Theor. Math. Phys. **90**, 219 (1992).
[11] M. Kardar, G. Parisi, and Y.-C. Zhang, Phys. Rev. Lett. **56**, 889 (1986).
[12] S. F. Edwards and D. R. Wilkinson, Proc. R. Soc. London, Ser. A **381**, 17 (1982).
[13] J. Garcia-Ojalvo and J. M. Sancho, *Noise in Spatially Extended Systems* (Springer, Berlin, 1999).
[14] S. N. Majumdar, A. J. Bray, and G. C. M. A. Ehrhardt, Phys. Rev. E **64**, 015101(R) (2001).
[15] C. Dasgupta, M. Constantin, S. Das Sarma, and S. N. Majumdar, Phys. Rev. E **69**, 022101 (2004).
[16] N.-N. Pang, Y.-K. Yu, and T. Halpin-Healy, Phys. Rev. E **52**, 3224 (1995).
[17] F. Family, J. Phys. A **19**, L441 (1986).
[18] J. M. Kim and J. M. Kosterlitz, Phys. Rev. Lett. **62**, 2289 (1989).
[19] W. H. Press *et al.*, *Numerical Recipes* (Cambridge University, Cambridge, England, 1989).
[20] J. Buceta, J. Pastor, M. A. Rubio, and F. J. de la Rubia, Phys. Rev. E **61**, 6015 (2000).
[21] S. Das Sarma, S. V. Ghaisas, and J. M. Kim, Phys. Rev. E **49**, 122 (1994).
[22] W. W. Mullins, J. Appl. Phys. **28**, 333 (1957); C. Herring, *ibid.* **21**, 301 (1950).